

Multi-Objective Multi-Agent Planning for Discovering and Tracking Multiple Mobile Objects

Hoa Van Nguyen, Ba-Ngu Vo, Ba-Tuong Vo, Hamid Rezaatofghi and Damith C. Ranasinghe

Abstract—We consider the online planning problem for a team of agents with on-board sensors to discover and track an unknown and time-varying number of moving objects from sensor measurements with uncertain measurement-object origins. Since the onboard sensors have limited field of views (FoV), the usual planning strategy based solely on either tracking detected objects or discovering unseen objects is inadequate. To address this, we formulate a new multi-objective multi-agent model for a predictive control problem based on information-theoretic criteria; cast as a partially observable Markov decision process (POMDP). The resulting multi-agent planning problem is exponentially complex due to the unknown data association between objects and multi-sensor measurements; hence, computing an optimal control action is intractable. We prove that the proposed multi-objective value function is a monotone submodular set function, and develop a greedy algorithm that can achieve an 0.5OPT compared to an optimal algorithm. We demonstrate the proposed solution via a series of numerical experiments with a real-world dataset.

Index Terms—Multi-object tracking, random finite sets, multi-agent control, submodular, MM-POMDP.

I. INTRODUCTION

Recent advancements in robotics have inspired applications that use low-cost mobile sensors (*e.g.*, drones) ranging from vision-based surveillance, threat detection via (chemical, biological, radiological and nuclear) source localisation, search and rescue, to wildlife monitoring [23]. At the heart of these applications is Multi-Object Tracking (MOT)—the task of estimating an unknown and time-varying number of objects and their trajectories from sensor measurements. Although a single agent can be tasked with MOT, such a system is limited by its observability, computing resources and energy. Using multi-agents alleviates these problems, improves synergy and affords robustness to failures. Further, MOT is fundamental for autonomous operation as it provides awareness of the dynamic environment the agents operate in. Realising this potential requires the multi-agents to collaborate and operate autonomously.

In this work, we consider the challenging problem of coordinating multi-agents to *simultaneously* seek *undetected objects*

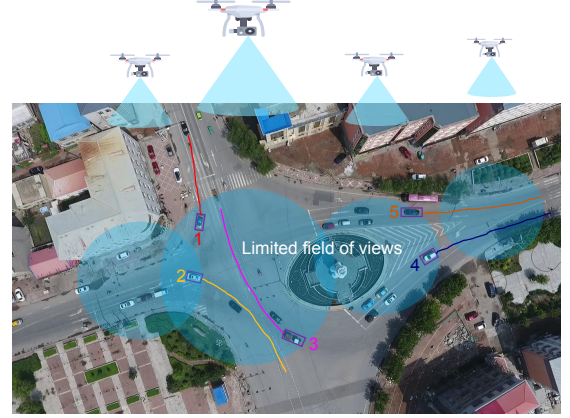


Fig. 1. A UAV team deployed to search and track multiple vehicles of interest with limited field of view sensors where measurements to object associations are unknown but must be consistent across the team to reason and plan for tracking and searching for vehicles of interest.¹

and track *detected objects* (see Fig. 1). Tracking involves estimating trajectories of objects and maintaining their provisional identities or labels. Trajectories are important for capturing the behaviour of objects while labels provide the means for distinguishing individual trajectories and for human/machine users to communicate information on the relevant trajectories. Discovering undetected objects and tracking detected objects are two competing objectives due to the limited field-of-view (FoV) of the sensors (*e.g.* cameras, antenna, and radar) and the random appearance/disappearance of objects. On one hand, following only detected objects to track them accurately means that many undetected objects could be missed. On the other hand, leaving detected objects to explore unseen regions for undetected objects will lead to track loss. Thus, the problem of seeking *undetected objects* and tracking *detected objects* is a multi-objective optimisation problem.

Even for standard state-space models, where the system state (and measurement) is a finite-dimensional vector, multi-agent planning with multiple competing objectives is challenging due to complex interactions between agents resulting in combinatorial optimisation problems [34]. In MOT, where the system state (and measurement) is a set of vectors, the problem is further complicated due to: *i*) the unknown and time-varying number of trajectories; *ii*) missing and false detections; and *iii*) unknown data association [20]. Most critically for real-world applications, multi-agent control actions must be computed online and in a timely manner.

Meta-heuristics (so-called bio-inspired) techniques such as genetic algorithms and particle swarm optimisation are ex-

Acknowledgement: This work is supported by the Australian Research Council under LP160101177, LP200301507, and FT210100506 Projects. .

Hoa Van Nguyen, Ba-Tuong Vo and Ba-Ngu Vo are with the Department of Electrical and Computer Engineering, Curtin University, Bentley, WA 6102, Australia (e-mail: hoa.v.nguyen,ba-tuong.vo,ba-ngu.vo@curtin.edu.au).

Hamid Rezaatofghi is with the Department of Data Science & AI, Monash University, Clayton VIC 3800, Australia (e-mail: hamid.rezaatofghi@monash.edu).

Damith C. Ranasinghe is with the School of Computer Science, The University of Adelaide, SA 5005, Australia (e-mail: damith.ranasinghe@adelaide.edu.au).

¹The inset images are extracted from the VisDrone-2019 dataset [9].

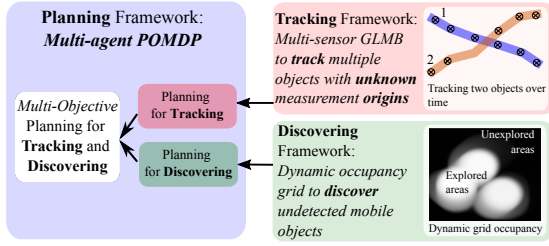


Fig. 2. A schematic of the proposed planning approach.

pensive for real-time applications in dynamic environments such as MOT, especially for multi-agents. On the other hand, the model predictive control (MPC) approach is effective in autonomous control systems and is widely used in real-world applications [11]. In particular, the MPC problem can be cast as a partially observed Markov decision process (POMDP), which has been gaining significant interests as a real-time planning approach [3]. The cooperation problem amongst agents can be formulated as a decentralised POMDP (Dec-POMDP), whose exact solutions are NEXP-hard [2]. Moreover, for multi-agent POMDPs, the action and observation space grows exponentially with the number of agents, and hence not suitable for real-time applications. So far, the centralised MPOMDP approach [21] offers a more tractable alternative for coordinating multiple agents [7], [33], and hence, adopted in this work.

Computing optimal control actions for MOT within a POMDP requires a suitable framework that provides a multi-object density that serves as the information state. Hence, amongst various MOT algorithms, we adopt the labelled random finite set (RFS) multi-object filtering framework for its ability to: *i*) conveniently provide the multi-object filtering density (that contains all information on the current set of trajectories); and *ii*) address the time-varying set of labelled trajectories of the mobile objects. Single-agent planning with RFS filters has been studied in with unlimited FoV [13], [28] and extended to multi-agent planning using distributed fusion techniques [33]. However, these multi-agent planning methods are only suitable when the agents have an unlimited detection range [25]. A multi-agent POMDP with an RFS filter was proposed in [7] for searching and localisation, but not tracking.

To achieve competing detection and tracking objectives, we propose a POMDP with a multi-objective value function consisting of information gains for both detected and undetected objects, as shown in Fig. 2. A simple solution for competing objective functions is to weigh and add them together. However, meaningful weighting parameters are difficult to determine. A multi-objective optimisation approach naturally provides a meaningful trade-off between competing objectives. To the best of our knowledge, multi-agent planning for MOT with a multi-objective value function has not been investigated. The first multi-objective POMDP with an RFS filter was proposed in [36] for a sensor selection problem.

For MOT and the computation of the information state, we use the multi-sensor Generalised Labelled Multi-Bernoulli (MS-GLMB) filter [30] a *linear* computational complexity in the total number of measurements across sensors. Further, to

reduce computation time for planning, we propose approximating the differential-entropy-based value function by replacing the information state, which is a GLMB density with a simpler LMB density that matches the first moment and cardinality distribution. We show that the approximate value functions for POMDP can be computed analytically, thereby enabling sub-optimal multi-agents control actions to be determined in a timely manner. In summary, the main contributions are:

- 1) a multi-objective POMDP formulation for multi-agent planning to search and track multi-objects;
- 2) an efficient multi-agent path planning algorithm based on differential entropy.

The proposed method is evaluated using the **CRAWDAD taxi dataset** [8] on multi-UAVs control for searching and tracking an unknown and time-varying number of taxis in downtown San Francisco, USA. For performance benchmarking, our preliminary work in [24] is used as the ideal or best-case scenarios where data association is known.

The remainder of this paper is organised as follows. Section II provides relevant background for our MOT and planning framework. Section III presents our proposed multi-objective value function for the control of the multi-agent to simultaneously track and discover objects. Section IV evaluates our proposed method on a real-world dataset. Section V summarises our contributions and discusses future directions.

II. BACKGROUND

This section presents the problem statement, as well as the necessary background on random finite sets the MS-GLMB filter and MPOMDP.

A. Problem statement

Consider a team of agents, identified by a set of unique labels $\mathcal{N} = \{1, \dots, |\mathcal{N}|\}$, monitoring a spatial area $G \subset \mathbb{R}^{d_x}$ to search and track a time-varying and unknown number of moving objects. The agents can self-localise (*e.g.*, using on-board GPS sensors) and are equipped with range-limited and homogeneous sensors that register measurements with *unknown data associations* (*i.e.*, the unknown measurement-to-object origin). The agents can communicate to a central node (*e.g.*, send measurements to a central node for processing), while the central node can compute and send control actions to the agents [7]. We assume that conditional on the ensemble of object states, the measurements obtained by individual agents are independent [29]².

Throughout, we follow the notation used in [32]. Lowercase letters (*e.g.*, x, \mathbf{x}) denote the state vectors of individual objects, referred to as single-object states. States augmented with labels are bolded to distinguish them from unlabelled ones. Uppercase letters (*e.g.*, X, \mathbf{X}) denote sets of single-object states at a given time, referred to as multi-object states. Spaces and labelled spaces are denoted by blackboard uppercase letters (*e.g.*, \mathbb{X}, \mathbb{L}) and bold blackboard uppercase letters (*e.g.*, \mathbf{X}, \mathbf{U}), respectively. For a given set S , $\mathcal{F}(S)$, $|S|$, $1_S(\cdot)$, $\delta_S[\cdot]$

²This assumption holds if there is no interference among agents when getting measurements.

denote, respectively, the class of finite subsets, cardinality, indicator function, and (generalised) Kronecker delta function, of S ($\delta_S[X] = 1$, if $X = S$, and zero otherwise). For a given function f , its multi-object exponential f^X is defined as $\prod_{x \in X} f(x)$, with $f^\emptyset = 0$. The inner product $\int f(x)g(x)dx$ is written as $\langle f, g \rangle$.

B. Bayesian Multi-object Estimation

A random finite set (RFS) model [17], [19] succinctly captures the random nature of the multi-object state, and also provides its probability density as the information state for the POMDP. An RFS X of a state-space \mathbb{X} is a random variable taking values in $\mathcal{F}(\mathbb{X})$, and is commonly characterised by Mahler's multi-object density [19] (see also subsection II-C). Since the elements of multi-object states in this work are distinctly labelled, we use a *labelled RFS* model. Given an RFS X of \mathbb{X} and a (discrete) label space \mathbb{L} , a labelled RFS \mathbf{X} is an RFS of $\mathbf{X} \triangleq \mathbb{X} \times \mathbb{L}$ constructed by marking the elements of X with distinct labels from \mathbb{L} [32].

In a Bayesian filtering context, the (labelled) multi-object filtering density at the current time k (conditioned the observation history up to time k) contains all information on the ensemble of states and their trajectories [32]. For compactness, the subscript k for the current time is omitted, and the next time $k+1$ is denoted by $+$. Analogous to the standard Bayes filter, the multi-object filtering density is propagated forward in time via the multi-object Bayes filter

$$\pi_+(\mathbf{X}_+) \propto g(\mathbf{Z}_+|\mathbf{X}_+) \int f_+(\mathbf{X}_+|\mathbf{X}) \pi(\mathbf{X}) \delta \mathbf{X}, \quad (1)$$

where: π , π_+ and \mathbf{X} , \mathbf{X}_+ are the multi-object filtering densities and multi-object states at the current and next times; g and f_+ are the multi-object observation likelihood and transition density; the integral is Mahler's set integral. The multi-object observation likelihood g captures the detections, false alarms, occlusions, and misdetections. The multi-object transition density f_+ captures the motions as well as births and deaths of objects.

C. Generalized Labeled Multi-Bernoulli Filtering

For an agent with label $n \in \mathcal{N}$, we denote $\mathbf{U}^{(n)} \triangleq \mathbb{U} \times \{n\}$, $\mathbf{A}^{(n)} \triangleq \mathbb{A} \times \{n\}$, and $\mathbf{Z}^{(n)} \triangleq \mathbb{Z} \times \{n\}$. For simplicity, assume that all agents have the same common agent-state space³ $\mathbf{U} \triangleq \mathbb{U} \times \mathcal{N}$, a common discrete control action space $\mathbf{A} \triangleq \mathbb{A} \times \mathcal{N}$ (e.g., $\mathbb{A} = \{\rightarrow, \searrow, \downarrow, \swarrow, \leftarrow, \nwarrow, \uparrow, \nearrow\}$), and a common measurement space (homogenous sensors) $\mathbf{Z} \triangleq \mathbb{Z} \times \mathcal{N}$. Given a set \mathbf{X} of objects, each $\mathbf{x} \in \mathbf{X}$ has probability $P_D(\mathbf{x}, \mathbf{u})$ of being detected by an agent with state $\mathbf{u} = (u, n) \in \mathbf{U}$, and generates an observation $\mathbf{z} = (z, n') \in \mathbf{Z}$ with likelihood [18]:

$$g(\mathbf{z}|\mathbf{x}, \mathbf{u}) = \delta_n[n']g(z|\mathbf{x}, u, n) = \delta_n[n']g^{(n)}(z|\mathbf{x}, u), \quad (2)$$

or missed with probability $1 - P_D(\mathbf{x}, \mathbf{u})$. The term $\delta_n[n']$ ensures that measurements generated by agent (with label) n

are tagged with the same label. The observation set $\mathbf{Z}^{(n)} = \{(z_1, n), \dots, (z_{|\mathbf{Z}^{(n)}|}, n)\} \in \mathcal{F}(\mathbf{Z})$ at agent n , is formed by the superposition of the (object-originated) detections and Poisson clutter with intensity $\kappa(\mathbf{z}|\mathbf{u}) = \delta_n[n']\kappa(z|u, n) = \delta_n[n']\kappa^{(n)}(z|u)$. It is standard practice to assume that conditional on \mathbf{X} , detections are independent of each other and clutter [19], and that the measurements obtained by individual agents are independent [29]. The multi-agent observation can be expressed as the disjoint union $\mathbf{Z} \triangleq \mathbf{Z}^{(1)} \uplus \dots \uplus \mathbf{Z}^{(|\mathcal{N}|)}$ $\in \mathcal{F}(\mathbf{Z})$ ⁴ or equivalently as the array $\mathbf{Z} \triangleq (\mathbf{Z}^{(1)}, \dots, \mathbf{Z}^{(|\mathcal{N}|)})$.

Remark 1: The detection probability, clutter rate and measurement likelihood always depend on the agent-state \mathbf{u} . For notational simplicity, \mathbf{u} will usually be suppressed unless otherwise stated, i.e., $P_D(\mathbf{x}, \mathbf{u}, n) \triangleq P_D^{(n)}(\mathbf{x})$, $\kappa(\mathbf{z}, n|\mathbf{u}, n) \triangleq \kappa^{(n)}(\mathbf{z})$, and $g(\mathbf{z}, n|\mathbf{x}, \mathbf{u}, n) \triangleq g^{(n)}(\mathbf{z}|\mathbf{x})$.

The objects are mapped to the multi-agent observation by a multi-agent *association map* γ , where individual elements in $\mathbf{Z}^{(n)}$ are associated with objects via the *positive 1-1 map*⁵ $\gamma^{(n)}: \mathbb{L} \rightarrow \{-1: |\mathbf{Z}^{(n)}|\}$, and $\gamma^{(1)}(\ell) = \dots = \gamma^{(|\mathcal{N}|)}(\ell) = -1$ if ℓ is a dead/unborn label [30]. Here $\gamma^{(n)}(\ell) = -1$ means object ℓ does not exist, $\gamma^{(n)}(\ell) = 0$ means object ℓ is not detected by agent n , and $\gamma^{(n)}(\ell) > 0$ means object ℓ generates observation $\mathbf{z}_{\gamma^{(n)}(\ell)}$ at agent n [32]. The positive 1-1 property ensures each observation from agent n originates from at most one object, and the set $\mathcal{L}(\gamma) \triangleq \{\ell \in \mathbb{L} : \gamma^{(1)}(\ell), \dots, \gamma^{(|\mathcal{N}|)}(\ell) \geq 0\}$ is called the *live labels* of γ . The space of all such multi-agent association is denoted as Γ .

The Bayes recursion (1) admits an analytical filtering density in the form of a Generalised Labelled Multi-Bernoulli (GLMB) [32]:

$$\pi(\mathbf{X}) = \Delta(\mathbf{X}) \sum_{I, \xi} w^{(I, \xi)} \delta_I[\mathcal{L}(\mathbf{X})] [p^{(\xi)}]^{\mathbf{X}}, \quad (3)$$

where $I \in \mathcal{F}(\mathbb{L})$, $\xi \triangleq \gamma_{1:k} \in \Xi$, the space of all (multi-agent) association histories up to the current time, each $w^{(I, \xi)}$ is non-negative such that $\sum_{I, \xi} w^{(I, \xi)} = 1$, and each $p^{(\xi)}(\cdot, \ell)$ is a probability density on \mathbb{X} . For convenience, a GLMB is represented by the set of components

$$\pi \triangleq \left\{ \left(w^{(I, \xi)}, p^{(\xi)} \right) : (I, \xi) \in \mathcal{F}(\mathbb{L}) \times \Xi \right\}. \quad (4)$$

Under the standard multi-object system model [19], if the current filtering density is the GLMB (4), then the filtering density at the next time is a GLMB given by the *MS-GLMB recursion* [30]

$$\pi_+ = \Omega(\pi; \mathbf{Z}_+). \quad (5)$$

Consequently, if the initial prior is a GLMB, then all subsequent filtering densities are GLMBs. A GLMB density $\pi(\cdot)$ can be approximated by an LMB $\hat{\pi}(\cdot)$ with the same moment and cardinality distribution [27], given by:

$$\hat{\pi}(\mathbf{X}) = \Delta(\mathbf{X}) \tilde{r}^{\mathbb{L} - \mathcal{L}(\mathbf{X})} r^{\mathcal{L}(\mathbf{X})} p^{\mathbf{X}}, \quad (6)$$

where $r^{(\ell)} = \sum_{(I, \xi) \in \mathcal{F}(\mathbb{L}) \times \Xi} 1_I(\ell) w^{(I, \xi)}$, $\tilde{r}^{(\cdot)} = 1 - r^{(\cdot)}$, and $p^{(\ell)}(x) = \frac{1}{r^{(\ell)}} \sum_{(I, \xi) \in \mathcal{F}(\mathbb{L}) \times \Xi} 1_I(\ell) w^{(I, \xi)} p^{(\xi)}(x, \ell)$ are,

³The measurement errors of agents' internal actuator-sensor are assumed negligible, thus the agent state is known.

⁴Since all sensors are assumed to be homogeneous, it is sufficient to represent the multi-sensor measurement space as $\mathcal{F}(\mathbf{Z})$.

⁵No two distinct arguments are mapped to the same positive value.

respectively, the existence probability of object ℓ , and its the probability density. An LMB is completely characterised by the parameter set $\{r^{(\ell)}, p^{(\ell)}(\cdot)\}_{\ell \in \mathbb{L}}$.

D. Multi-agent POMDP (MPOMDP)

A partition matroid of the action space $\mathbf{A}^{(n)}$ is a collection of subsets of $\mathbf{A}^{(n)}$, defined by [5]:

$$\mathcal{M} = \{\mathbf{A} \subseteq \mathbf{A}^{(n)} : |\mathbf{A} \cap \mathbf{A}^{(n)}| \leq 1 \ \forall n \in \mathcal{N}\}. \quad (7)$$

A set \mathbf{A} of actions with $|\mathbf{A} \cap \mathbf{A}^{(n)}| = 1$ is said to be complete for agent n . If $|\mathbf{A} \cap \mathbf{A}^{(n)}| = 0$ then \mathbf{A} is said to be incomplete for agent n . The partition matroid construct ensures that each agent n can only select at *most* one control action from its local control action space $\mathbf{A}^{(n)}$.

A centralised multi-agent POMDP for tracking multi-objects can be characterised by the tuple $(\mathcal{N}, H, \mathcal{F}(\mathbf{X}), \mathcal{F}(\mathbf{Z}), \mathcal{F}(\mathbf{U}), \mathcal{M}, f_+, g, \varrho)$, where:

- \mathcal{N} is the finite set of agent labels;
- H is the look-ahead time horizon;
- $\mathcal{F}(\mathbf{X})$ is the labelled multi-object state space;
- $\mathcal{F}(\mathbf{Z})$ is the common observation space of the all agents (assumed to have homogeneous sensors);
- $\mathcal{F}(\mathbf{U})$ is the common state space of all agents;
- \mathcal{M} is the partition matroid of all actions of all agents;
- $f_+ : [\mathcal{F}(\mathbf{X}) \times \mathcal{F}(\mathbf{U})] \times [\mathcal{F}(\mathbf{X}) \times \mathcal{F}(\mathbf{U})] \times \mathcal{M} \rightarrow [0, \infty)$ denotes the transition kernel $f_+((\mathbf{X}_+, \mathbf{U}_+) | (\mathbf{X}, \mathbf{U}), \mathbf{A})$;
- $g : \mathcal{F}(\mathbf{Z}) \times [\mathcal{F}(\mathbf{X}) \times \mathcal{F}(\mathbf{U})] \times \mathcal{M} \rightarrow [0, \infty)$ denotes the joint observation likelihood function $g(\mathbf{Z}_+(\mathbf{A}) | (\mathbf{X}_+, \mathbf{U}_+(\mathbf{A})), \mathbf{A})$;
- $\varrho : [\mathcal{F}(\mathbf{X}) \times \mathcal{F}(\mathbf{U})] \times \mathcal{M} \times \mathcal{F}(\mathbf{Z}) \rightarrow \mathbb{R}$ denotes the immediate reward $\varrho((\mathbf{X}, \mathbf{U}(\mathbf{A})), \mathbf{A}, \mathbf{Z}(\mathbf{A}))$ for being in state $(\mathbf{X}, \mathbf{U}(\mathbf{A}))$ after performing action $\mathbf{A} \in \mathcal{M}$ which results in measurement $\mathbf{Z}(\mathbf{A})$.

The coordination of the agents is realised via the control action $\mathbf{A} \in \mathcal{M}$. Each $\mathbf{a}^{(n)} \in \mathbf{A}$ at time k prescribes a trajectory $\mathbf{u}_{1:H}(\mathbf{a}^{(n)}) \triangleq (\mathbf{u}_{k+1}(\mathbf{a}^{(n)}), \dots, \mathbf{u}_{k+H}(\mathbf{a}^{(n)}))$ of positions for agent n on the interval $\{k+1, \dots, k+H\}$, along which it collects the multi-object measurement sequence $\mathbf{Z}_{1:H}(\mathbf{a}^{(n)}) \triangleq (\mathbf{Z}_{k+1}(\mathbf{a}^{(n)}), \dots, \mathbf{Z}_{k+H}(\mathbf{a}^{(n)}))$. For convenience, we denote $\mathbf{X}_{1:H} \triangleq (\mathbf{X}_{k+1}, \dots, \mathbf{X}_{k+H})$, $\mathbf{U}_{1:H}(\mathbf{A}) \triangleq (\mathbf{U}_{k+1}(\mathbf{A}), \dots, \mathbf{U}_{k+H}(\mathbf{A}))$, $\mathbf{Z}_{1:H}(\mathbf{A}) \triangleq (\mathbf{Z}_{k+1}(\mathbf{A}), \dots, \mathbf{Z}_{k+H}(\mathbf{A}))$, where $\forall j \in \{k+1, \dots, k+H\}$: $\mathbf{U}_j(\mathbf{A}) \triangleq \mathbf{u}_{\mathbf{a} \in \mathbf{A}} \mathbf{u}_j(\mathbf{a})$, $\mathbf{Z}_j(\mathbf{A}) \triangleq \mathbf{z}_{\mathbf{a} \in \mathbf{A}} \mathbf{Z}_j(\mathbf{a})$.

A POMDP seeks, at time k , the control action(s) $\mathbf{A} \in \mathcal{M}$ that maximises the the *value function*:

$$V(\mathbf{X}_{1:H}, \mathbf{U}_{1:H}(\mathbf{A}), \mathbf{A}, \mathbf{Z}_{1:H}(\mathbf{A})) \triangleq \mathbb{E} \left[\sum_{j=k+1}^{k+H} \varrho(\mathbf{X}_j, \mathbf{U}_j(\mathbf{A}), \mathbf{A}, \mathbf{Z}_j(\mathbf{A})) \right], \quad (8)$$

which is the expected sum of immediate rewards $\varrho(\cdot)$ over horizon H . Here, $\mathbb{E}[\cdot]$ denotes the expected operator.

Remark 2: The value function $V(\cdot)$ always depends on the agents' positions \mathbf{U} and action \mathbf{A} . Hereafter,

for simplicity, \mathbf{U} and \mathbf{A} are suppressed, *e.g.*, $V(\mathbf{X}_{1:H}, \mathbf{U}_{1:H}(\mathbf{A}), \mathbf{A}, \mathbf{Z}_{1:H}(\mathbf{A})) \triangleq V(\mathbf{X}_{1:H}, \mathbf{Z}_{1:H}(\mathbf{A}))$; $\varrho(\mathbf{X}_j, \mathbf{U}_j(\mathbf{A}), \mathbf{A}, \mathbf{Z}_j(\mathbf{A})) \triangleq \varrho(\mathbf{X}_j, \mathbf{Z}_j(\mathbf{A}))$.

In general, analytic solutions to POMDP in (8) are not available while numerical solutions (*e.g.*, using Monte Carlo integration in [23]) are computationally intractable/intensive, especially for multiple agents. Alternatively, a computationally tractable value-function based on the notion of predicted ideal measurement set (PIMS) [19], *i.e.*,

$$V(\mathbf{X}_{1:H}, \widehat{\mathbf{Z}}_{1:H}(\mathbf{A})) = \sum_{j=k+1}^{k+H} \varrho(\mathbf{X}_j, \widehat{\mathbf{Z}}_j(\mathbf{A})). \quad (9)$$

where the predicted ideal measurement set $\widehat{\mathbf{Z}}_j(\mathbf{A})$ is constructed by generating measurements from the predicted multi-object state without measurement noise, clutter nor misdetection. When no confusion arises, we denote $V(\mathbf{X}_{1:H}, \widehat{\mathbf{Z}}_{1:H}(\mathbf{A}))$ as $V(\mathbf{A})$.

III. PLANNING FOR TRACKING AND DISCOVERING MULTIPLE OBJECTS

This section presents our approach to multi-agent planning for searching, detecting and tracking an unknown and time-varying number of objects, with limited FoV sensors. This problem is very challenging due to: *i*) undetected objects resulting from the limited FoVs; *ii*) unknown locations of objects without any prior information; *iii*) unknown measurement-object origins and unknown and time-varying number of objects; and *iv*) the combinatorial nature in computing the control actions for multiple agents. An overview of the proposed solution is illustrated in Fig. 2.

A. Differential Entropy and Mutual Information

We begin by extending the concepts of differential entropy [6, pp.243], and mutual information [6, pp.251] to RFS. Differential entropy is commonly used to measure information uncertainty while and mutual information commonly used to measure the information content of one random variable in another. These concepts are needed to formulate the objectives for our multi-agent POMDP, as well as the derivation of tractable solutions. To define meaningful differential entropy and mutual information for RFS, we need to take a closer look at the notion of probability density for RFS.

The probability density $f : \mathcal{F}(\mathbb{X}) \rightarrow [0, \infty)$, of an RFS X , is taken w.r.t. the reference measure μ defined for each measurable $\mathcal{T} \subseteq \mathcal{F}(\mathbb{X})$ by:

$$\mu(\mathcal{T}) = \sum_{i=0}^{\infty} \frac{1}{i!K^i} \int 1_{\mathcal{T}}(\{x_1, \dots, x_i\}) d(x_1, \dots, x_i),$$

where K is the unit of hyper-volume on \mathbb{X} , $1_{\mathcal{T}}(\cdot)$ is the indicator function for \mathcal{T} , and by convention the integral for $i=0$ is $1_{\mathcal{T}}(\emptyset)$. Note that the probability density f and the reference measure μ are unitless. The role of μ is analogous to the Lebesgue measure on \mathbb{X} , and the integral of a function $f : \mathcal{F}(\mathbb{X}) \rightarrow [0, \infty)$ w.r.t. μ :

$$\int f(X) \mu(dX) = \sum_{i=0}^{\infty} \frac{1}{i!K^i} \int f(\{x_1, \dots, x_i\}) d(x_1, \dots, x_i).$$

Note that this integral is equivalent to Mahler's set integral [19], defined for a function π by

$$\int \pi(X) \delta X = \sum_{i=0}^{\infty} \frac{1}{i!} \int \pi(\{x_1, \dots, x_i\}) d(x_1, \dots, x_i),$$

in the sense that $\int K^{-|X|} f(X) \delta X = \int f(X) \mu(dX)$. Hence, $K^{-|X|} f(X)$ is Mahler's Finite Set Statistics (FISST) density.

Analogous to random variables, differential entropy and mutual information for RFS are defined as follows.

Definition 1: The differential entropy $h(X)$ of a random finite set X , described by a probability density f_X , is defined as

$$h(X) = - \int f_X(Y) \ln(f_X(Y)) \mu(dY). \quad (10)$$

Remark 3: Using the equivalence with Mahler's set integral, the differential entropy of an RFS X , with (FISST) density π_X , can be written as

$$h(X) = - \int \pi_X(Y) \ln(K^{|Y|} \pi_X(Y)) \delta Y. \quad (11)$$

Definition 2: The mutual information between the RFSs X and Z is defined as

$$I(X; Z) = h(X) - h(X|Z), \quad (12)$$

where $h(X|Z) = \int h(X|Z = \zeta) \pi_Z(\zeta) \delta \zeta$, and $\pi_Z(\cdot)$ is the (FISST) density of Z .

For an LMB RFS, see (6), the differential entropy can be expressed analytically as follows

Proposition 1: The differential entropy of an LMB X , with parameter set $\{r^{(\ell)}, p^{(\ell)}(\cdot)\}_{\ell \in \mathbb{L}}$ is

$$h(X) = - \sum_{\ell \in \mathbb{L}} \left[r^{(\ell)} \ln r^{(\ell)} + \tilde{r}^{(\ell)} \ln \tilde{r}^{(\ell)} + r^{(\ell)} \left\langle p^{(\ell)} \ln(K p^{(\ell)}) \right\rangle \right]. \quad (13)$$

Note that when each single-object density is a Gaussian mixture (i.e., $p^{(\ell)}(x) = \sum_{i=1}^{N_i} \alpha_i^{(\ell)} \mathcal{G}(x; m_i^{(\ell)}, \Sigma_i^{(\ell)})$), we can approximate $p^{(\ell)}(x) \approx \mathcal{G}(x; \bar{m}^{(\ell)}, \bar{\Sigma}^{(\ell)})$, where

$$\bar{m}^{(\ell)} = \sum_{i=1}^{N_i} \alpha_i^{(\ell)} m_i^{(\ell)}, \bar{\Sigma}^{(\ell)} = \sum_{i=1}^{N_i} \alpha_i^{(\ell)} \left[\Sigma_i^{(\ell)} + (m_i^{(\ell)} - \bar{m}^{(\ell)})(m_i^{(\ell)} - \bar{m}^{(\ell)})^T \right].$$

Consequently, $-\langle p^{(\ell)} \ln(K p^{(\ell)}) \rangle \approx 0.5 \ln[\det(2\pi e \bar{\Sigma}^{(\ell)})]$, and (13) can be approximated as:

$$h(X) \approx - \sum_{\ell \in \mathbb{L}} \left[r^{(\ell)} \ln r^{(\ell)} + \tilde{r}^{(\ell)} \ln \tilde{r}^{(\ell)} - 0.5 r^{(\ell)} \ln[\det(2\pi e \bar{\Sigma}^{(\ell)})] \right].$$

Remark 4: The result in Proposition 1 significantly reduces the computational complexity of computing the differential entropy of an LMB X from $\mathcal{O}(2^{\mathbb{L}})$ to $\mathcal{O}(\mathbb{L})$. As a result, the computational complexity of computing $h(X)$ is *linearly proportional* to the number of objects.

Remark 5: A special case of the above proposition is the differential entropy of a Bernoulli RFS, i.e. an LMB with only one component, parameterised by (r, p) :

$$h(X) = -[r \ln(r) + \tilde{r} \ln \tilde{r} + r \langle p \ln(K p) \rangle].$$

Optimising the value function of a realistic POMDP is computationally intensive if not intractable. Fortunately, when

the value function is a *monotone submodular* set function, sub-optimal solutions can be computed using a greedy algorithm with drastically lower complexity [14], [26]. In the following we establish monotone submodularity of mutual information, see proof in Appendix VI.

Definition 3: [22]. A set function $q: \mathcal{F}(\mathbf{A}) \rightarrow \mathbb{R}$, i.e. a real-valued function whose domain is the class of finite subsets of a given set, is said to be *monotone* if $q(\mathbf{A}) \leq q(\mathbf{B}) \forall \mathbf{A} \subseteq \mathbf{B} \subseteq \mathbf{A}$, and *submodular* if $q(\mathbf{B} \cup \{\mathbf{a}\}) - q(\mathbf{B}) \leq q(\mathbf{A} \cup \{\mathbf{a}\}) - q(\mathbf{A})$, $\forall \mathbf{A} \subseteq \mathbf{B} \subseteq \mathbf{A}, \forall \mathbf{a} \in \mathbf{A} \setminus \mathbf{B}$.

Proposition 2: Suppose that conditioned on the multi-object state, the measurements collected by the agents are conditionally independent from each other. Given a set $\mathbf{A} \in \mathcal{F}(\mathbf{A})$ of actions, let $q_I(\mathbf{A}) \triangleq I(\mathbf{X}; \mathbf{Z}(\mathbf{A}))$ denote the mutual information between the multi-object state \mathbf{X} (with density π_X) and measurement $\mathbf{Z}(\mathbf{A})$ (with density $\pi_{Z(\mathbf{A})}$) collected by the agents when the actions in \mathbf{A} are taken. Then $q_I(\cdot)$ is a monotone submodular set function on $\mathcal{F}(\mathbf{A})$.

B. Planning for tracking

This subsection presents the information-based value function for the tracking task. The rationale is that optimising the information content of the information state would improve tracking accuracy. Our approach does not require defining the value function as an expectation. Inspired by the PIMS approach in [19] (see (9)), we propose using a novel value function via the mutual information $I(\mathbf{X}; \hat{\mathbf{Z}})$ between the multi-object state \mathbf{X} and the *ideal* measurement state $\hat{\mathbf{Z}}$. Here, $\hat{\mathbf{Z}}$ is generated from \mathbf{X} without data association (i.e., known as the measurement-object assignment), as well as without measurement noise, clutters or misdetections. The value function is defined as

$$V_1(\mathbf{A}) = \sum_{j=k+1}^{k+H} I(\mathbf{X}_j; \hat{\mathbf{Z}}_j(\mathbf{A})), \quad (14)$$

where $I(\mathbf{X}; \hat{\mathbf{Z}}) = h(\mathbf{X}) - h(\mathbf{X}|\hat{\mathbf{Z}})$; $h(\cdot)$ defined in (13).

Corollary 3: The value function $V_1(\mathbf{A})$ in (14) is a monotone submodular set function.

Proof: From Proposition 2, $I(\mathbf{X}; \hat{\mathbf{Z}}(\mathbf{A}))$ is a monotone submodular set function and $V_1(\mathbf{A})$ is a positive linear combination of it. Hence, it follows from [22, pp.272], $V_1(\mathbf{A})$ is a monotone submodular set function. \square

C. Planning for discovery

1) Occupancy grid for undetected objects.: Some objects of interest can be outside of sensor's FoVs, and thus cannot be detected. However, the knowledge of undetected objects outside the sensor's FoVs is usually not exploited.

In this work, we develop an occupancy grid to capture the knowledge about undetected objects outside sensor's FoV. Intuitively, the knowledge of unexplored regions can be incorporated into the planning to increase the likelihood of discovering new objects. In contrast to *static* occupancy grids for *stationary* objects in [29], a *dynamic* occupancy grid is proposed by including the probability of each grid cell containing at least one undetected *mobile* object, namely the

discovery probability. We divide the search area of interest G into an occupancy grid, i.e., $G = \mathcal{X}^{(1)} \cup \dots \cup \mathcal{X}^{(N_{\mathcal{X}})} \subset \mathbb{R}^{d_{\mathcal{X}}}$. Further, we define a pair $(r_{\mathcal{X}}^{(i)}, \mathcal{X}_c^{(i)})$ to be associated with $\mathcal{X}^{(i)}$ such that $\mathcal{X}_c^{(i)} \in \mathcal{X}^{(i)}$ denotes the centre point of cell $\mathcal{X}^{(i)}$, and $r_{\mathcal{X}}^{(i)} \in [0, 1]$ denotes the discovery probability, i.e. the probability that the occupancy cell $\mathcal{X}^{(i)}$ contains at least one *undetected mobile object*. For any cell $\mathcal{X}^{(i)} \subset G$, since undetected objects may or may not be present in $\mathcal{X}^{(i)}$, we model the occupancy state in cell $\mathcal{X}^{(i)}$ by the Bernoulli RFS $X^{(i)}$ whose state can be either \emptyset or $\{\mathcal{X}_c^{(i)}\}$. When $X^{(i)}$ is empty, it is *not* occupied with probability $\tilde{r}_{\mathcal{X}}^{(i)}$. When $X^{(i)}$ is not empty, it is occupied (by undetected objects) with probability $r_{\mathcal{X}}^{(i)}$. The density of the Bernoulli RFS $X^{(i)}$ is given by

$$\pi(X^{(i)}) = \begin{cases} \tilde{r}_{\mathcal{X}}^{(i)}, & \text{if } X^{(i)} = \emptyset, \\ r_{\mathcal{X}}^{(i)}, & \text{if } X^{(i)} = \{\mathcal{X}_c^{(i)}\}. \end{cases} \quad (15)$$

The problem of computing the grid occupancy of undetected objects in cell $\mathcal{X}^{(i)}$ is equivalent to that of tracking a stationary object located at the centroid of cell $\mathcal{X}_c^{(i)}$, wherein our goal is to determine the probability $r_{\mathcal{X}}^{(i)}$. Hence, we apply the multi-sensor Bernoulli filter (MS-BF) in [31] to compute $r_{\mathcal{X}}^{(i)}$ over time using the *empty measurements*⁶. Specially, suppose $r_{\mathcal{X}}^{(i)}$ and $r_{\mathcal{X},+}^{(i)}$ are the probability at time k and $k+1$ respectively, we have:

$$r_{\mathcal{X},+}^{(i)} = \Psi(|\mathcal{N}|) \circ \dots \circ \Psi^{(1)}(\tilde{r}_{\mathcal{X}}^{(i)} r_{\mathcal{X},B}^{(i)} + r_{\mathcal{X}}^{(i)} P_S(\mathcal{X}_c^{(i)})),$$

$$[\Psi^{(n)}(r_{\mathcal{X}}^{(i)})] = \frac{(1 - P_{D,+}^{(n)}(\mathcal{X}_c^{(i)})) r_{\mathcal{X}}^{(i)}}{\tilde{r}_{\mathcal{X}}^{(i)} + r_{\mathcal{X}}^{(i)} (1 - P_{D,+}^{(n)}(\mathcal{X}_c^{(i)}))} \quad (16)$$

where $P_S(\cdot)$ and $P_{D,+}^{(n)}(\cdot)$ are the same survival and detection probabilities defined in subsection II-C, $r_{\mathcal{X},B}^{(i)}$ is the birth probability, i.e. the probability of undetected objects appearing/entering the cell $\mathcal{X}^{(i)}$. At initial time $k=0$, we can set $r_{\mathcal{X},0}^{(i)} = r_{\mathcal{X},B}^{(i)}$ if there is no prior information. From (16), the discovery probability $r_{\mathcal{X}}^{(i)}$ depends on the detection probability $P_{D,+}^{(n)}(\mathcal{X}_c^{(i)})$ —a function of the location of sensor n (see Remark 1) and the centre point $\mathcal{X}_c^{(i)}$ —which conforms with our intuition.

2) *Planning for discovery:* This subsection presents our information-based value function for the discovery task. The rationale is to increase the multi-agent's chances of detecting undetected objects by maximising the mutual information amongst the occupancy grid cells G and the empty measurement set \mathbf{Z}^{\emptyset} . Since the measurement set is empty, the expected operator in (8) no longer has an effect, i.e.,

$$V_2(\mathbf{A}) = \sum_{j=k+1}^{k+H} I(G_k; \mathbf{Z}_j^{\emptyset}(\mathbf{A})), \quad (17)$$

where $I(G_k; \mathbf{Z}_j^{\emptyset}(\mathbf{A})) = \mathcal{H}(G_k) - \mathcal{H}(G_k | \mathbf{Z}_j^{\emptyset}(\mathbf{A}))$, $\mathcal{H}(G_k)$ is the Shannon entropy (a discrete version of differential entropy $h(\cdot)$) of G_k . Since each grid cell $\mathcal{X}^{(i)}$ is associated

with a Bernoulli random variable $r_{\mathcal{X},k}^{(i)} \in (0, 1)$, according to Remark 5, we have:

$$\mathcal{H}(G_k) = - \sum_{i=1}^{N_{\mathcal{X}}} [r_{\mathcal{X},k}^{(i)} \ln(r_{\mathcal{X},k}^{(i)}) + \tilde{r}_{\mathcal{X},k}^{(i)} \ln(\tilde{r}_{\mathcal{X},k}^{(i)})],$$

and $\mathcal{H}(G_k | \mathbf{Z}_j^{\emptyset}(\mathbf{A}))$ follows the exact form as $\mathcal{H}(G_k)$ except that $r_{\mathcal{X},j}^{(i)}$ is computed by propagating $r_{\mathcal{X},k}^{(i)}$ from k to j with the *empty measurement* $\mathbf{Z}_j^{\emptyset}(\mathbf{A})$.

Proposition 4: The value function V_2 in (17) is a monotone submodular set function.

Proof: Following the same strategy in Proposition 2, we can prove that $I(G_k; \mathbf{Z}_j^{\emptyset}(\mathbf{A}))$ is a monotone submodular set function. Additionally, $V_2(\mathbf{A})$ is a positive linear combination of $I(G_k; \mathbf{Z}_j^{\emptyset}(\mathbf{A}))$, thus $V_2(\mathbf{A})$ is a monotone submodular set function according to [22, pp.272]. \square

D. Planning for tracking and discovering objects using a multi-objective value function

To control a team of agents to track and discover, we consider the multi-objective value function

$$V(\mathbf{A}) = [V_1(\mathbf{A}), V_2(\mathbf{A})]^T, \quad (18)$$

where $\mathbf{A} \in \mathcal{M}$, while V_1 and V_2 are respectively described in (14) and (17). Multi-objective optimisation provides a meaningful notion of trade-off amongst objectives via the Pareto-set, wherein no solutions can improve one objective without degrading the other remaining ones. Additionally, online planning requires choosing a solution from Pareto-set in a timely manner. One possible method is robust submodular observation selection (ROSS) [16] which selects a robust solution against the worst possible objective; however, the resulting value function is usually not submodular. Other alternative methods are the global criterion method (GCM) and weighted sum (WS), which are simple and retain the submodularity of the two value functions. Therefore, we choose GCM [15] to compute a trade-off solution by examining the distance of these two value functions from an ideal solution. The resulting value function from GCM is V_{mo} (with $V_{mo}(\emptyset) = 0$), given by:

$$V_{mo}(\mathbf{A}) = \sum_{i=1}^2 \frac{V_i(\mathbf{A}) - \min_{\mathbf{A} \in \mathcal{M}} V_i(\mathbf{A})}{\max_{\mathbf{A} \in \mathcal{M}} V_i(\mathbf{A}) - \min_{\mathbf{A} \in \mathcal{M}} V_i(\mathbf{A})}. \quad (19)$$

According to [4], GCM yields a unique solution. Thus, the multi-objective optimisation problem turns into

$$\mathbf{A}^* = \arg \max_{\mathbf{A} \in \mathcal{M}} V_{mo}(\mathbf{A}). \quad (20)$$

In principle, computing an optimal control action \mathbf{A}^* is a combinatorial optimisation problem, unless $V_{mo}(\mathbf{A})$ is a monotone submodular set function; hence, a greedy algorithm can be implemented to reduce computational time. To this end, we have the following result:

Corollary 5: V_{mo} in (19) is also a monotone submodular set function.

⁶Since objects are undetected, the measurements from the undetected objects are empty.

Algorithm 1 Greedy search algorithm

```

1: Input:  $\mathcal{M}, V_{mo}$  ▷ action space and value function.
2: Output:  $A_g \in \mathcal{M}$  ▷ greedy control action.
3:  $A_g := \emptyset$  ▷ initialise empty greedy control action.
4:  $P := \emptyset$  ▷ initialise empty planned agent's list.
5:  $U := \mathcal{N}$  ▷ initialise planning agent's list.
6: while  $U \neq \emptyset$  do
7:   for each  $n \in U$  do
8:      $[a_g^{(n)}, V_c^{(n)}] := \arg \max_{a \in \mathbf{A}^{(n)}} V_{mo}(A_g \uplus a)$ 
9:   end for
10:   $n^* := \arg \max_{n \in U} V_c^{(n)}$  ▷  $n^*$  that yields the best value function.
11:   $A_g := A_g \uplus a_g^{(n^*)}$  ▷ store action with agent  $n^*$ .
12:   $P := P \cup \{n^*\}$  ▷ add  $n^*$  into planned agent's list.
13:   $U := U \setminus \{n^*\}$  ▷ delete  $n^*$  from planning agents' list.
14: end while

```

Proof: From Corollary 3 and Proposition 4, $V_1(\mathbf{A})$ and $V_2(\mathbf{A})$ are both monotone submodular set functions. Since $V_{mo}(\mathbf{A})$ is a positive linear combination of $V_1(\mathbf{A})$ and $V_2(\mathbf{A})$, thus $V_{mo}(\mathbf{A})$ is a monotone submodular set function, according to [22, pp.272]. \square

E. Greedy search algorithm

Let OPT denote the optimal value of a submodular function subject to a partition matroid \mathcal{M} , *i.e.*, $\text{OPT} = \max_{\mathbf{A} \in \mathcal{M}} V_{mo}(\mathbf{A})$. Since $V_{mo}(\cdot)$ is a monotone submodular set function (Corollary 5), it follows from [10] that a solution from a greedy search algorithm yields a lower bound performance at 0.5OPT (see Proposition 6).

Proposition 6: Let A_g be the control action computed from a greedy search algorithm and $\text{OPT} = \max_{\mathbf{A} \in \mathcal{M}} V_{mo}(\mathbf{A})$. Then we have:

$$V_{mo}(A_g) \geq 0.5\text{OPT}. \quad (21)$$

The above result justifies implementing a greedy search algorithm by including individual agents sequentially and selecting the next best agents that maximise the value function $V_{mo}(\cdot)$, as shown in Algorithm 1.

IV. EVALUATIONS OVER A REAL-WORLD DATASET

To demonstrate the performance of our proposed method, we conduct simulated experiments using the CROWDAD taxi dataset [8] which contains several traces of taxis within a 6150 m \times 6080 m area in San Francisco Bay Area, USA. In particular, we randomly selected 10 taxi tracks over 1000 s (from 18-May-2008 4:43:20 PM to 18-May-2008 5:00:00 PM), as shown in Fig. 3. Inspired by the approach in [7], the search area is scaled down by a factor of 5, while the time is sped up by the same factor of 5 so that the taxi's speed remains the same as in the real world. Thus, the simulated environment has an area of 1230 m \times 1216 m and a total search time of 200 s.

Since taxis can go into different routes, we employ the constant turn (CT) model with an unknown turn rate to account for its turning behaviour. In particular, let $\mathbf{x} = (x, \ell) \in \mathbb{T}$ denote the single object state comprising the label ℓ and kinematics $\mathbf{x} = [\tilde{\mathbf{x}}^T, \theta]^T$ where $\tilde{\mathbf{x}} = [\rho_x, \dot{\rho}_x, \rho_y, \dot{\rho}_y]^T$ is its

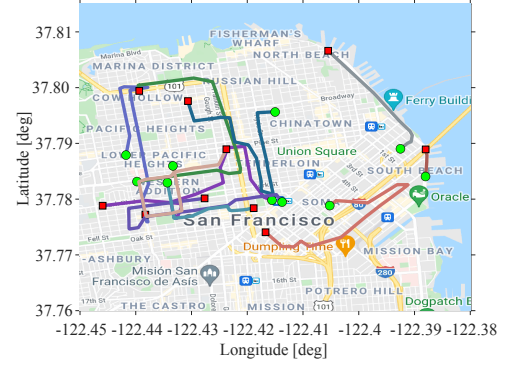


Fig. 3. CROWDAD taxi dataset. There are 10 taxis travelling within an area of 6150 m \times 6080 m in San Francisco Area over 1000 s. \circ/\square symbols denote Start/Stop positions of each taxi with different colours representing different taxis.

position and velocity in Cartesian coordinates, and θ is the turn rate. Each object follows a constant turn model given by

$$\tilde{\mathbf{x}}_{k+1|k} = F^{CT}(\theta_k) \tilde{\mathbf{x}}_k + G^{CT} \eta_k, \quad (22)$$

$$\theta_{k+1|k} = \theta_k + T_0 q_k \quad (23)$$

where $F^{CT}(\theta) = [1, 0, 0, 0; \sin(\theta T_0)/\theta, \cos(\theta T_0), (1 - \cos(\theta T_0))/\theta, \sin(\theta T_0); 0, 0, 1, 0; -(1 - \cos(\theta T_0))/\theta, -\sin(\theta T_0), \sin(\theta T_0)/\theta, \cos(\theta T_0)]^T$, $G^{CT} = [T_0^2/2, T_0, 0, 0; 0, 0, T_0^2/2, T_0]^T$ and $T_0 = 1$ s is a sampling interval; $\eta_k \sim \mathcal{G}(\cdot; 0, \sigma_\eta^2 I_2)$ with $\sigma_\eta = 0.15$ m/s² and I_2 is the 2×2 identity matrix; $q_k \sim \mathcal{G}(\cdot; 0, \sigma_q^2)$, and $\sigma_q^2 = \pi/60$ rad/s. The on-board sensor on each agent is range-limited subject to r_D and its detection probability follows:

$$P_D(\mathbf{x}, \mathbf{u}) = \begin{cases} P_D^{\max} & d(\mathbf{x}, \mathbf{u}) \leq r_D, \\ \max(0, P_D^{\max} - (d(\mathbf{x}, \mathbf{u}) - r_D)\bar{h}) & \text{otherwise,} \end{cases}$$

where $d(\mathbf{x}, \mathbf{u})$ is the distance between the object \mathbf{x} and agent \mathbf{u} . A noisy *position-based* sensor is considered in our experiments wherein a detected object \mathbf{x} yields a noisy position measurement \mathbf{z} , given by: $\mathbf{z} = [p_x, p_y]^T + \mathbf{v}$. Here, $\mathbf{v} \sim \mathcal{G}(0, R)$ with $R = \text{diag}(\sigma_x^2, \sigma_y^2)$. Notably, we selected parameters for our experiments based on the real-world experimental results in [12]. In particular, the minimum altitude of UAVs is 126 m, and its detection range is $r_D = 126$ m and $\bar{h} = 0.008$. The on-board sensor is corrupted by false-alarm measurements with a clutter rate $\lambda = 0.0223$, and a maximum detection probability of $P_D^{\max} = 0.8825$ (see Table VIII in [35]). We see that the estimation error from a UAV flying at 60 m altitude using a standard visual sensor is around 0.55 m [12]. Since our UAVs fly at higher altitude and the measurement noise is proportional to the UAV's altitude, we set our measurement noise $\sigma_x = \sigma_y = 0.55 \times 126/60 = 1.115$ m. Further, a total number of 10 UAVs (*e.g.*, quad-copters) are considered in this experiment, which depart at the centre of the search area, *i.e.*, $[615, 608, 126]^T$. Since there is no prior knowledge of each object's state, we model initial births at time $k = 0$ by a grid-based LMB density with parameters $\{(r_{B,0}^{(i)}, p_B^{(i)})\}_{i=1}^{N_B}$. Here, N_B is the number of birth parameters, $p_B^{(i)} = \mathcal{G}(\mathbf{x}; m_B^{(i)}, \Sigma_B)$ with $\Sigma_B = \text{diag}([\Delta_x/2; 1; \Delta_y/2; 1])^2$ and $m_B^{(i)} = [\rho_{B,x}^{(i)}, 0, \rho_{B,y}^{(i)}, 0]^T$ where the position elements

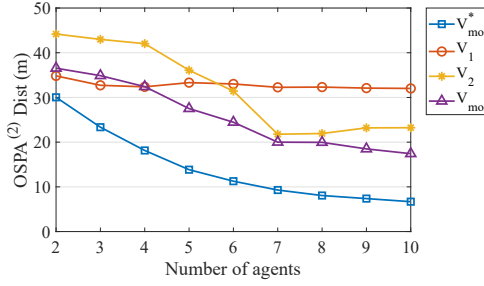


Fig. 4. Our multi-objective value function V_{mo} versus baseline methods over 100 Monte Carlo runs when $|\mathcal{N}|$ is increased from 2 to 10. V_{mo}^* is the best possible performance when the measurement origins are known.

$\rho = (\rho_{B,x}, \rho_{B,y})$ are grid cells of the search area with (Δ_x, Δ_y) spacing in $x - y$ directions. For the next time step, we propose an adaptive birth procedure that incorporates the current grid occupancy information at time k into the birth probability at the next time $k + 1$. Note that, since the number of occupancy grid cells $N_{\mathcal{X}}$ can be significantly large, which may impact the filtering time if there are too many birth parameters, we propose resizing the occupancy grid $\{(r_{\mathcal{X},+}^{(i)}, \mathcal{X}_c^{(i)})\}_{i=1}^{N_{\mathcal{K}}}$ to $\{(\bar{r}_{\mathcal{X}}^{(i)}, m_B^{(i)})\}_{i=1}^{N_B}$, with $N_B \ll N_{\mathcal{X}}$, using bicubic interpolation⁷ to efficiently improve the filtering time. The birth existence probability is then updated by:

$$r_{B,+}^{(i)} = \frac{[1 + \bar{r}_{\mathcal{X}}^{(i)} / \max(\bar{r}_{\mathcal{X}}^{(i)})] (\sum_{i=1}^{N_B} r_{B,0}^{(i)})}{\sum_{i=1}^{N_B} [1 + \bar{r}_{\mathcal{X}}^{(i)} / \max(\bar{r}_{\mathcal{X}}^{(i)})]}, \quad (24)$$

to ensure the number of expected births (i.e., $\sum_{i=1}^{N_B} r_{B,+}^{(i)}$) remains fixed over time.

For tracking performance evaluation, we use the optimal sub-pattern assignment (OSPA⁽²⁾) in [1] with cut-off $c = 50$ m, order $p = 1$, over a window length of the entire experimental duration. All results are averaged over 100 Monte Carlo runs. A smaller **OSPA⁽²⁾ Dist (m)** indicates a better tracking performance in localisation, cardinality, track fragmentation and track switching errors.

A. Performance over an increasing number of agents

In this subsection, the experiments are conducted to validate the hypothesis that our proposed multi-objective value function V_{mo} outperforms a single objective that either focuses on tracking or discovering in terms of overall tracking performance. Therefore, we examine the performance of three following planning algorithms: (i) utilising a single *tracking* objective value function V_1 , (ii) utilising a single *discovering* objective value function V_2 , (iii) utilising a multi-objective value function V_{mo} that simultaneously optimises both tracking and discovering tasks. Additionally, we also analyse $V_{mo}(\cdot)$ versus the previous multi-objective value function $V_{mo}^*(\cdot)$ when the data association (measurement-to-object origin) is known [24], which can be considered as the best possible (upper bound) performance.

Fig. 4 shows tracking performance in terms of **OSPA⁽²⁾ Dist** for tracking 10 taxis in CRAWDAD taxi dataset when

⁷In particular, we can use `imresize` — a common MATLAB command to resize images using bicubic interpolation.

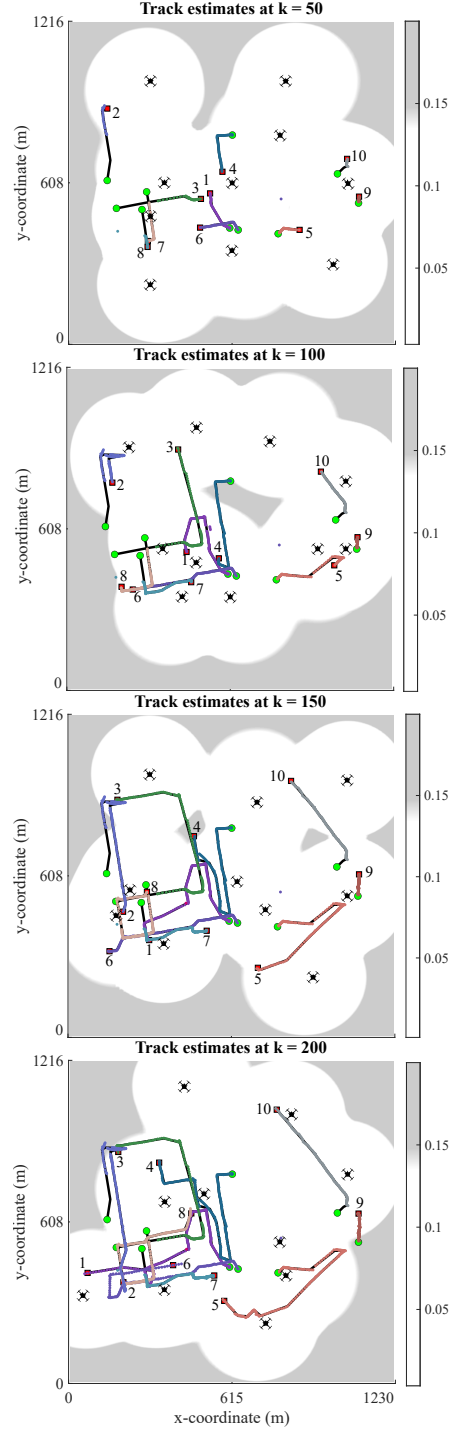


Fig. 5. A particular run using V_{mo} . **Background:** grid occupancy probability. **Foreground:** estimated and true positions of 10 taxis. Black solid lines denote the ground truths of taxi's trajectories, while the coloured dot points denote the estimated positions of taxis. Different colours denote different identities of estimated taxis. \circ/\square symbols denote Start/Stop positions of each taxi. The drone symbol denotes UAV's positions.

the number of agents increases from 2 to 10. On the one hand, when the number of agents is small (less than four), we observe that our V_1 achieves a similar accuracy as our V_{mo} since there are not enough agents to cover the area, the team should focus on tracking objects instead of exploring. On the other hand, when the number of agents is large (more

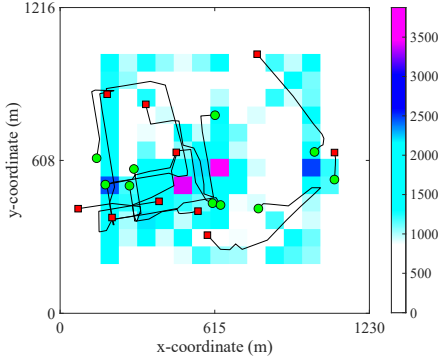


Fig. 6. The heatmap (16×16 grids) of trajectories for 10 UAVs over 100 MC runs using V_{mo} . \circ/\square symbols denote the Start/Stop positions of each object. The colour bar denotes the number of times UAVs' positions inside a grid cell.

than four), our proposed multi-objective value function V_{mo} constantly outperforms V_1 and V_2 , since there are enough agents to perform both tracking and discovering tasks simultaneously. As expected, the tracking objective V_1 does not improve tracking performance when the number of agents increases since V_1 only focuses on tracking detected objects and misses out detecting and tracking objects outside of their FoVs.

B. Detailed Experimental Results

In this subsection, we provide detailed results to further demonstrate the effectiveness and insights of our method when the number of UAVs is 10. Fig. 5 depicts the estimated trajectories versus the true trajectories of 10 taxi traces in the foreground, and the grid occupancy probability in the background, for the CRAWDAID taxi dataset in a particular run using our proposed V_{mo} control method over time. The results demonstrate that we can correctly search and track all taxis with correct identities (different colours denote different taxis).

Fig. 6 further shows the the trajectory's heatmap for 10 UAVs over 100 MC runs. The outcome shows that our control method V_{mo} navigates 10 UAVs to concentrate more in the western region of the area of interest where there are more taxis around, while also slightly covering the eastern region to successfully track the remaining taxis. It is expected that as time increases, the agents start to spread out from the centre to cover more area, which helps to detect and track more taxis.

Fig. 7 details the overall mean and standard deviation ($\mu \pm 0.2\sigma$) to search and track 10 taxi traces for different control methods for 10 UAVs in terms of OSPA⁽²⁾ Dist, OSPA⁽²⁾ Loc, OSPA⁽²⁾ Card as well as the number of estimated taxis (*i.e.*, Cardinality) over 100 MC runs. The results show that our proposed V_{mo} consistently outperforms the tracking-only V_1 or discovering-only V_2 in terms of the overall tracking performance (*i.e.*, OSPA⁽²⁾ Dist) over time. Further, for localisation error (*i.e.*, OSPA⁽²⁾ Loc), the performance of V_{mo} approaches the performance of the ideal case V_{mo}^* . Additionally, we observe that most control methods can estimate the number of taxis (*i.e.*, Cardinality) correctly, except V_1 which

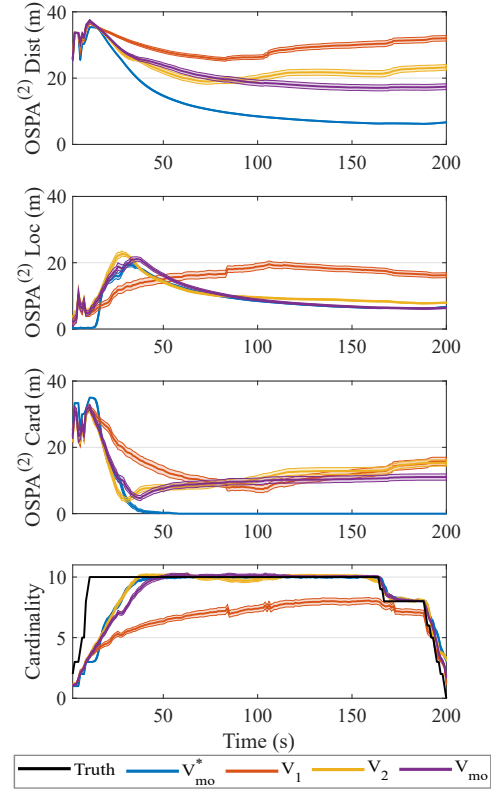


Fig. 7. The overall tracking performance ($\mu \pm 0.2\sigma$) over time over 100 MC runs using different control methods.

only focuses on tracking and does not explore to find any taxis outside of the team's FoVs. In terms of OSPA⁽²⁾ Card, which considers not only the cardinality estimates but also the track label switching and track fragmentation, we also observe that V_{mo} outperforms V_1 and V_2 . Notably, since the cardinality is estimated correctly, most OSPA⁽²⁾ Card errors come from the track label switching and track fragmentation errors, which is expected given the limited FoV sensors, and the motion model mismatch between the CT model and the taxi's occasional turns.

V. CONCLUSION

We have developed a multi-objective planning method for discovering and tracking multiple mobile objects for multi-agents with unknown data associations. The proposed multi-objective value function is shown to be monotone and sub-modular, thereby enabling low-cost implementation via greedy search. A series of experiments on a real-world taxi dataset confirm our method's capability and efficiency. It also validates our proposed multi-objective method's robustness, wherein its overall performance shows decreasing trend over time similar to that of the best possible performance. So far, we have considered a centralised MPOMDP for multi-agent planning where scalability can be a limitation. A scalable approach should be a distributed POMDP for MOT, where each agent runs its local filter to track multi-objects and coordinates with other agents to achieve a global objective. However, planning for multi-agents to reach a global goal under a distributed POMDP framework is a NEXP-complete problem [2].

REFERENCES

- [1] M. Beard, B. T. Vo, and B.-N. Vo. A solution for large-scale multi-object tracking. *Trans. on Sig. Proc.*, 2020. IV
- [2] D. S. Bernstein, R. Givan, N. Immerman, and S. Zilberstein. The complexity of decentralized control of Markov decision processes. *Math. of Op. Research*, 27(4):819–840, 2002. I, V
- [3] J. B. Clempner and A. S. Poznyak. Observer and control design in partially observable finite Markov chains. *Automatica*, 110:108587, 2019. I
- [4] C. A. C. Coello, G. B. Lamont, D. A. Van Veldhuizen, et al. *Evolutionary algorithms for solving multi-objective problems*, volume 5. Springer, 2007. III-D
- [5] M. Corah and N. Michael. Distributed submodular maximization on partition matroids for planning on large sensor networks. In *Proc. of CDC*, pages 6792–6799, 2018. II-D
- [6] T. M. Cover and J. A. Thomas. *Elements of information theory*. John Wiley & Sons, 2012. III-A, III-A, VI, VI
- [7] P. Dames, P. Tokekar, and V. Kumar. Detecting, localizing, and tracking an unknown number of moving targets using a team of mobile robots. *The Inter. J. of Rob. Res.*, 36(13-14):1540–1553, 2017. I, II-A, IV
- [8] [dataset] M. Piorkowski, N. Sarafijanovic-Djukic, and M. Grossglauser. CRAWDAD dataset epfl/mobility (v. 2009-02-24). Downloaded from <https://crawdad.org/epfl/mobility/20090224>, Feb. 2009. I, IV
- [9] [dataset] P. Zhu, L. Wen, D. Du, X. Bian, H. Fan, Q. Hu, and H. Ling. Detection and tracking meet drones challenge. *Trans. on Pat. Ana. and Mach. Intel.*, pages 1–20, 2021. I
- [10] M. L. Fisher, G. L. Nemhauser, and L. A. Wolsey. An analysis of approximations for maximizing submodular set functions—II. In *Poly. Comb.*, pages 73–87. Springer, 1978. III-E
- [11] C. E. Garcia, D. M. Prett, and M. Morari. Model predictive control: Theory and practice—A survey. *Automatica*, 1989. I
- [12] G. Guido, V. Gallelli, D. Rogano, and A. Vitale. Evaluating the accuracy of vehicle tracking data obtained from unmanned aerial vehicles. *Inter. J. of Transport. Sci. and Tech.*, 5(3):136–151, 2016. IV
- [13] H. G. Hoang and B. T. Vo. Sensor management for multi-target tracking via multi-Bernoulli filtering. *Automatica*, 50(4):1135–1142, 2014. I
- [14] S. T. Jawaid and S. L. Smith. Submodularity and greedy algorithms in sensor scheduling for linear dynamical systems. *Automatica*, 61:282–288, 2015. III-A
- [15] J. Koski. Multicriterion structural optimization. In *Optimization of Large Structural Systems*, pages 793–809. Springer Netherlands, Dordrecht, 1993. III-D
- [16] A. Krause, H. B. McMahan, C. Guestrin, and A. Gupta. Robust submodular observation selection. *J. of Mac. Learn. Res.*, 9(Dec):2761–2801, 2008. III-D
- [17] W. Liu, S. Zhu, C. Wen, and Y. Yu. Structure modeling and estimation of multiple resolvable group targets via graph theory and multi-Bernoulli filter. *Automatica*, 89, 2018. II-B
- [18] R. Mahler. A GLMB filter for unified multitarget multisensor management. In *Sig. Proc., Sens./Info. Fusion, and Target Rec. XXVIII*, volume 11018, page 110180D, 2019. II-C
- [19] R. P. Mahler. *Statistical multisource-multitarget information fusion*. Artech House, 2007. II-B, II-B, II-C, II-C, II-D, III-A, III-B
- [20] R. P. Mahler. *Advances in statistical multisource-multitarget information fusion*. Artech House, 2014. I, VI
- [21] J. V. Messias, M. Spaan, and P. U. Lima. Efficient offline communication policies for factored multiagent POMDPs. In *Proc. of 24th NeurIPS*, pages 1917–1925, 2011. I
- [22] G. L. Nemhauser, L. A. Wolsey, and M. L. Fisher. An analysis of approximations for maximizing submodular set functions—I. *Math. Prog.*, 14(1):265–294, 1978. 3, III-B, III-C2, III-D
- [23] H. V. Nguyen, M. Chesser, L. P. Koh, H. Rezaatofghi, and D. C. Ranasinghe. TrackerBots: Autonomous unmanned aerial vehicle for real-time localization and tracking of multiple radio-tagged animals. *J. of F. Rob.*, 36(3), 2019. I, II-D
- [24] H. V. Nguyen, H. Rezaatofghi, B.-N. Vo, and D. C. Ranasinghe. Multi-objective multi-agent planning for jointly discovering and tracking mobile objects. In *Proc. of 34th AAAI*, pages 7227–7235, Feb 2020. I, IV-A
- [25] H. V. Nguyen, H. Rezaatofghi, B.-N. Vo, and D. C. Ranasinghe. Distributed Multi-object Tracking under Limited Field of View Sensors. *Trans. on Sig. Proc.*, 2021. I
- [26] G. Qu, D. Brown, and N. Li. Distributed greedy algorithm for multi-agent task assignment problem with submodular utility functions. *Automatica*, 105:206–215, 2019. III-A
- [27] S. Reuter, B.-T. Vo, B.-N. Vo, and K. Dietmayer. The labeled multi-Bernoulli filter. *Trans. on Sig. Proc.*, 62(12):3246–3260, 2014. II-C
- [28] B. Ristic and B.-N. Vo. Sensor control for multi-object state-space estimation using random finite sets. *Automatica*, 46(11):1812–1818, 2010. I
- [29] S. Thrun, W. Burgard, and D. Fox. *Probabilistic robotics*. MIT Press, 2005. II-A, II-C, III-C1
- [30] B. Vo, B. Vo, and M. Beard. Multi-sensor multi-object tracking with the generalized labeled multi-bernoulli filter. *Trans. on Sig. Proc.*, 67(23):5952–5967, Dec 2019. I, II-C, II-C
- [31] B. T. Vo, C. M. See, N. Ma, and W. T. Ng. Multi-sensor joint detection and tracking with the Bernoulli filter. *Trans. on Aero. and Elect. Sys.*, 48(2):1385–1402, 2012. III-C1
- [32] B.-T. Vo and B.-N. Vo. Labeled random finite sets and multi-object conjugate priors. *Trans. on Sig. Proc.*, 2013. II-A, II-B, II-B, II-C, II-C, VI, VI
- [33] X. Wang, R. Hoseinnezhad, A. K. Gostar, T. Rathnayake, B. Xu, and A. Bab-Hadiashar. Multi-sensor control for multi-object Bayes filters. *Sig. Proc.*, 142:260–270, 2018. I
- [34] S. Welikala, C. G. Cassandras, H. Lin, and P. J. Antsaklis. A new performance bound for submodular maximization problems and its application to multi-agent optimal coverage problems. *Automatica*, 144:110493, 2022. I
- [35] J. Zhu, K. Sun, S. Jia, Q. Li, X. Hou, W. Lin, B. Liu, and G. Qiu. Urban traffic density estimation based on ultrahigh-resolution UAV video and deep neural network. *J. of Sel. Top. in App. E. Obs. and Re. Sens.*, 11(12):4968–4981, 2018. IV
- [36] Y. Zhu, J. Wang, and S. Liang. Multi-objective optimization based multi-Bernoulli sensor selection for multi-target tracking. *Sensors*, 19(4):980 – 997, 2019. I

VI. APPENDIX - MATHEMATICAL PROOFS

Lemma 1: For $f : \mathcal{F}(\mathbb{L}) \rightarrow \mathbb{R}$, and $g : \mathbb{L} \rightarrow \mathbb{R}$, we have:

$$\sum_{L \subseteq \mathbb{L}} f(L) \sum_{\ell \in L} g(\ell) = \sum_{\ell \in \mathbb{L}} g(\ell) \sum_{L \subseteq \mathbb{L} \setminus \{\ell\}} f(L \cup \{\ell\}) \quad (25)$$

Proof: We will prove this Lemma via induction. It is trivial to confirm that (25) holds for $\mathbb{L} = \emptyset$ and $\mathbb{L} = \{\ell\}$.

Suppose (25) holds for $\mathbb{L} = \{\ell_1, \dots, \ell_n\}$, we need to prove that (25) also holds for $\mathbb{L} \cup \{\ell\}$, i.e.:

$$\sum_{L \subseteq \mathbb{L} \cup \hat{\ell}} f(L) \sum_{\ell \in L} g(\ell) = \sum_{\ell \in \mathbb{L} \cup \hat{\ell}} g(\ell) \sum_{L \subseteq \mathbb{L} \cup \hat{\ell} \setminus \{\ell\}} f(L \cup \{\ell\}). \quad (26)$$

Note that for any function $f : \mathcal{F}(\mathbb{L}) \rightarrow \mathbb{R}$, we have

$$\sum_{L \subseteq \mathbb{L} \cup \hat{\ell}} f(L) = \sum_{L \subseteq \mathbb{L}} f(L) + \sum_{L \subseteq \mathbb{L}} f(L \cup \{\ell\}) \quad (27)$$

since the subsets of $\mathbb{L} \cup \hat{\ell}$ are those subsets L of \mathbb{L} and those subsets $L \cup \{\ell\}$ where L are subsets of \mathbb{L} . Hence, we have:

$$\begin{aligned} & \sum_{L \subseteq \mathbb{L} \cup \hat{\ell}} f(L) \sum_{\ell \in L} g(\ell) \\ &= \sum_{L \subseteq \mathbb{L}} f(L) \sum_{\ell \in L} g(\ell) + \sum_{L \subseteq \mathbb{L}} f(L \cup \{\ell\}) \sum_{\ell \in L \cup \{\ell\}} g(\ell) \end{aligned} \quad (28)$$

Substituting (25) into (28), and note that $\sum_{\ell \in L \cup \{\ell\}} g(\ell) = \sum_{\ell \in L} g(\ell) + g(\ell)$, we have:

$$\begin{aligned}
& \sum_{L \subseteq \mathbb{L} \cup \hat{\ell}} f(L) \sum_{\ell \in L} g(\ell) \\
&= \sum_{\ell \in \mathbb{L}} g(\ell) \sum_{L \subseteq \mathbb{L} \setminus \{\ell\}} f(L \cup \{\ell\}) + \sum_{L \subseteq \mathbb{L}} f(L \cup \{\hat{\ell}\}) \sum_{\ell \in L} g(\ell) \\
&\quad + \sum_{L \subseteq \mathbb{L}} f(L \cup \{\hat{\ell}\}) g(\hat{\ell}) \\
&= \sum_{\ell \in \mathbb{L}} g(\ell) \sum_{L \subseteq \mathbb{L} \setminus \{\ell\}} f(L \cup \{\ell\}) \\
&\quad + \sum_{\ell \in \mathbb{L}} g(\ell) \sum_{L \subseteq \mathbb{L} \setminus \{\ell\}} f(L \cup \{\ell\} \cup \{\ell\}) + g(\hat{\ell}) \sum_{L \subseteq \mathbb{L}} f(L \cup \{\hat{\ell}\}) \\
&= \sum_{\ell \in \mathbb{L}} g(\ell) \sum_{L \subseteq \mathbb{L} \cup \hat{\ell} \setminus \{\ell\}} f(L \cup \{\ell\}) + g(\hat{\ell}) \sum_{L \subseteq \mathbb{L}} f(L \cup \{\hat{\ell}\}) \\
&= \sum_{\ell \in \mathbb{L} \cup \hat{\ell}} g(\ell) \sum_{L \subseteq \mathbb{L} \cup \hat{\ell} \setminus \{\ell\}} f(L \cup \{\ell\}) \quad \square.
\end{aligned}$$

Lemma 2: For $f : \mathcal{F}(\mathbb{L}) \rightarrow \mathbb{R}$, and $g : \mathbb{L} \rightarrow \mathbb{R}$, we have:

$$\sum_{L \subseteq \mathbb{L}} f(L) \sum_{\ell \in \mathbb{L} \setminus L} g(\ell) = \sum_{\ell \in \mathbb{L}} g(\ell) \sum_{L \subseteq \mathbb{L} \setminus \{\ell\}} f(L). \quad (29)$$

Proof: We will prove this Lemma via induction. It is trivial to confirm that (29) holds for $\mathbb{L} = \emptyset$ and $\mathbb{L} = \{\ell\}$. Suppose (29) holds for $\mathbb{L} = \{\ell_1, \dots, \ell_n\}$, we need to prove that (29) also holds for $\mathbb{L} \cup \{\ell\}$, i.e.:

$$\sum_{L \subseteq \mathbb{L} \cup \hat{\ell}} f(L) \sum_{\ell \in \mathbb{L} \cup \hat{\ell} \setminus L} g(\ell) = \sum_{\ell \in \mathbb{L} \cup \hat{\ell}} g(\ell) \sum_{L \subseteq \mathbb{L} \cup \hat{\ell} \setminus \{\ell\}} f(L). \quad (30)$$

Using the result of (27) and note that $\sum_{\ell \in \mathbb{L} \cup \{\hat{\ell}\} \setminus L} g(\ell) = \sum_{\ell \in \mathbb{L} \setminus L} g(\ell) + g(\hat{\ell})$, we have:

$$\begin{aligned}
& \sum_{L \subseteq \mathbb{L} \cup \hat{\ell}} f(L) \sum_{\ell \in \mathbb{L} \cup \hat{\ell} \setminus L} g(\ell) \\
&= \sum_{L \subseteq \mathbb{L}} f(L) \sum_{\ell \in \mathbb{L} \cup \hat{\ell} \setminus L} g(\ell) + \sum_{L \subseteq \mathbb{L}} f(L \cup \hat{\ell}) \sum_{\ell \in \mathbb{L} \setminus L} g(\ell) \\
&= \sum_{L \subseteq \mathbb{L}} f(L) \sum_{\ell \in \mathbb{L} \setminus L} g(\ell) + \sum_{L \subseteq \mathbb{L}} f(L) g(\hat{\ell}) + \sum_{L \subseteq \mathbb{L}} f(L \cup \hat{\ell}) \sum_{\ell \in \mathbb{L} \setminus L} g(\ell). \quad (31)
\end{aligned}$$

Substituting (29) into (31), we have:

$$\begin{aligned}
& \sum_{L \subseteq \mathbb{L} \cup \hat{\ell}} f(L) \sum_{\ell \in \mathbb{L} \cup \hat{\ell} \setminus L} g(\ell) \\
&= \sum_{\ell \in \mathbb{L}} g(\ell) \sum_{L \subseteq \mathbb{L} \setminus \{\ell\}} f(L) + g(\hat{\ell}) \sum_{L \subseteq \mathbb{L}} f(L) + \sum_{\ell \in \mathbb{L}} g(\ell) \sum_{L \subseteq \mathbb{L} \setminus \{\ell\}} f(L \cup \hat{\ell}) \\
&= \sum_{\ell \in \mathbb{L}} g(\ell) \sum_{L \subseteq \mathbb{L} \cup \hat{\ell} \setminus \{\ell\}} f(L) + g(\hat{\ell}) \sum_{L \subseteq \mathbb{L} \cup \hat{\ell} \setminus \{\ell\}} f(L) \\
&= \sum_{\ell \in \mathbb{L} \cup \hat{\ell}} g(\ell) \sum_{L \subseteq \mathbb{L} \cup \hat{\ell} \setminus \{\ell\}} f(L) \quad \square.
\end{aligned}$$

Lemma 3: For $f : \mathcal{F}(\mathbb{L}) \rightarrow \mathbb{R}$, $p : \mathbb{X} \times \mathbb{L} \rightarrow \mathbb{R}$, $q : \mathbb{X} \times \mathbb{L} \rightarrow \mathbb{R}$ with q is a unitless function, we have:

$$\int \Delta(\mathbf{X}) f(\mathcal{L}(\mathbf{X})) p^{\mathbf{X}} \ln q^{\mathbf{X}} \delta \mathbf{X} = \sum_{L \subseteq \mathbb{L}} f(L) \langle p \rangle^L \sum_{\ell \in L} \frac{\langle p \ln q \rangle(\ell)}{\langle p \rangle(\ell)}. \quad (32)$$

Proof: We have:

$$\int \Delta(\mathbf{X}) f(\mathcal{L}(\mathbf{X})) p^{\mathbf{X}} \ln q^{\mathbf{X}} \delta \mathbf{X} \quad (33)$$

$$= f(\emptyset) p^{\emptyset} \ln q^{\emptyset} + \sum_{i=1}^{\infty} \frac{1}{i!} \sum_{\ell_{1:i}} \delta_i[\{\ell_{1:i}\}] f(\{\ell_1, \dots, \ell_i\}) \times I, \quad (34)$$

$$= \sum_{i=1}^{\infty} \frac{1}{i!} \sum_{\ell_{1:i}} \delta_i[\{\ell_{1:i}\}] f(\{\ell_1, \dots, \ell_i\}) \times I, \quad (35)$$

where $I = \int \prod_{j=1}^i p(x_j, \ell_j) \ln \left(\prod_{n=1}^i q(x_n, \ell_n) \right) dx_{1:i}$.

Now, consider:

$$\begin{aligned}
I &= \int \prod_{j=1}^i p(x_j, \ell_j) \sum_{n=1}^i \ln q(x_n, \ell_n) dx_{1:i} \\
&= \sum_{n=1}^i \left(\int p(x_n, \ell_n) \ln [q(x_n, \ell_n)] dx_n \times \right. \\
&\quad \left. \prod_{j \in \{1, \dots, i\} \setminus \{n\}} \int p(x_j, \ell_j) dx_j \right) \\
&= \sum_{\ell \in \{\ell_{1:i}\}} \langle p \ln q \rangle(\ell) \langle p \rangle^{\{\ell_{1:i}\} - \{\ell\}}. \quad (36)
\end{aligned}$$

Since I is symmetric, substituting (36) into (35) and applying Lemma 12 in [32], we have:

$$\begin{aligned}
& \int \Delta(\mathbf{X}) f(\mathcal{L}(\mathbf{X})) p^{\mathbf{X}} \ln q^{\mathbf{X}} \delta \mathbf{X} \\
&= \sum_{i=1}^{\infty} \frac{1}{i!} \sum_{L: |L|=i} f(L) \left[\sum_{\ell \in L} \langle p \rangle^{L - \{\ell\}} \langle p \ln q \rangle(\ell) \right] \\
&= \sum_{L \subseteq \mathbb{L}} f(L) \langle p \rangle^L \sum_{\ell \in L} \frac{\langle p \ln q \rangle(\ell)}{\langle p \rangle(\ell)}.
\end{aligned}$$

Note that $f(\emptyset) \langle p \rangle^{\emptyset} \sum_{\ell \in \emptyset} \frac{\langle p \ln q \rangle(\ell)}{\langle p \rangle(\ell)} = 0$ due to sum over \emptyset \square .

Proof of Proposition 1: For the LMB density, we have $\pi(\mathbf{X}) = \Delta(\mathbf{X}) \tilde{r}^{\mathbb{L} \setminus \mathcal{L}(\mathbf{X})} r^{\mathcal{L}(\mathbf{X})} p^{\mathbf{X}}$; hence:

$$\begin{aligned}
-h(\mathbf{X}) &= \int \pi(\mathbf{X}) \ln (K^{|\mathbf{X}|} \pi(\mathbf{X})) \delta \mathbf{X} \\
&= \int \Delta(\mathbf{X}) \tilde{r}^{\mathbb{L} \setminus \mathcal{L}(\mathbf{X})} r^{\mathcal{L}(\mathbf{X})} p^{\mathbf{X}} \ln [\Delta(\mathbf{X}) \tilde{r}^{\mathbb{L} \setminus \mathcal{L}(\mathbf{X})} r^{\mathcal{L}(\mathbf{X})} p^{\mathbf{X}} K^{|\mathbf{X}|}] \delta \mathbf{X} \\
&= \int \Delta(\mathbf{X}) \tilde{r}^{\mathbb{L} \setminus \mathcal{L}(\mathbf{X})} r^{\mathcal{L}(\mathbf{X})} p^{\mathbf{X}} \ln [\tilde{r}^{\mathbb{L} \setminus \mathcal{L}(\mathbf{X})} r^{\mathcal{L}(\mathbf{X})}] \delta \mathbf{X} \\
&\quad + \int \Delta(\mathbf{X}) \tilde{r}^{\mathbb{L} \setminus \mathcal{L}(\mathbf{X})} r^{\mathcal{L}(\mathbf{X})} p^{\mathbf{X}} \ln [p^{\mathbf{X}} K^{|\mathbf{X}|}] \delta \mathbf{X}. \quad (37)
\end{aligned}$$

The first term of the RHS of (37) is:

$$\int \Delta(\mathbf{X}) \tilde{r}^{\mathbb{L} \setminus \mathcal{L}(\mathbf{X})} r^{\mathcal{L}(\mathbf{X})} p^{\mathbf{X}} \ln [\tilde{r}^{\mathbb{L} \setminus \mathcal{L}(\mathbf{X})} r^{\mathcal{L}(\mathbf{X})}] \delta \mathbf{X} \quad (38)$$

$$= \sum_{L \subseteq \mathbb{L}} \tilde{r}^{\mathbb{L} \setminus L} r^L \ln [\tilde{r}^{\mathbb{L} \setminus L} r^L] \left[\int p(x, \cdot) dx \right]^L \quad (39)$$

$$= \sum_{L \subseteq \mathbb{L}} \tilde{r}^{\mathbb{L} \setminus L} r^L \sum_{\ell \in \mathbb{L} \setminus L} \ln \tilde{r}^{(\ell)} + \sum_{L \subseteq \mathbb{L}} \tilde{r}^{\mathbb{L} \setminus L} r^L \sum_{\ell \in L} \ln r^{(\ell)} \quad (40)$$

$$= \sum_{\ell \in \mathbb{L}} \ln \tilde{r}^{(\ell)} \sum_{L \subseteq \mathbb{L} \setminus \{\ell\}} \tilde{r}^{\mathbb{L} \setminus L} r^L + \sum_{\ell \in \mathbb{L}} \ln r^{(\ell)} \sum_{L \subseteq \mathbb{L} \setminus \{\ell\}} \tilde{r}^{\mathbb{L} \setminus (L \cup \{\ell\})} r^{L \cup \{\ell\}} \quad (41)$$

$$= \sum_{\ell \in \mathbb{L}} \left[\tilde{r}^{(\ell)} \ln \tilde{r}^{(\ell)} \sum_{L \subseteq \mathbb{L} \setminus \{\ell\}} \tilde{r}^{(\mathbb{L} \setminus \{\ell\}) \setminus L} r^L + r^{(\ell)} \ln r^{(\ell)} \sum_{L \subseteq \mathbb{L} \setminus \{\ell\}} \tilde{r}^{(\mathbb{L} \setminus \{\ell\}) \setminus L} r^L \right] \quad (42)$$

$$= \sum_{\ell \in \mathbb{L}} \left[r^{(\ell)} \ln r^{(\ell)} + \tilde{r}^{(\ell)} \ln \tilde{r}^{(\ell)} \right]. \quad (43)$$

Here, (39) is the result of Lemma 3 in [32]; (40) is due to $\int p(x, \cdot) dx = 1$; Each term in (41) is the result of Lemma 2 and Lemma 1, respectively; while (43) is the result of the Binomial Theorem, i.e., $\sum_{L \subseteq \mathbb{L}} f^{\mathbb{L} \setminus L} g^L = (f + g)^{\mathbb{L}}$; hence, $\sum_{L \subseteq \mathbb{L} \setminus \{\ell\}} \tilde{r}^{(\mathbb{L} \setminus \{\ell\}) \setminus L} r^L = (\tilde{r} + r)^{\mathbb{L} \setminus \{\ell\}} = 1$.

The second term of the RHS of (37) is:

$$\int \Delta(\mathbf{X}) \tilde{r}^{\mathbb{L} \setminus \mathcal{L}(\mathbf{X})} r^{\mathcal{L}(\mathbf{X})} p^{\mathbf{X}} \ln [p^{\mathbf{X}} K^{|\mathbf{X}|}] \delta \mathbf{X} \quad (44)$$

$$= \sum_{L \subseteq \mathbb{L}} \tilde{r}^{\mathbb{L} \setminus L} r^L \sum_{\ell \in L} \left\langle p^{(\ell)} \ln(K p^{(\ell)}) \right\rangle \quad (45)$$

$$= \sum_{\ell \in \mathbb{L}} \left\langle p^{(\ell)} \ln(K p^{(\ell)}) \right\rangle \sum_{L \subseteq \mathbb{L} \setminus \{\ell\}} \tilde{r}^{\mathbb{L} \setminus (L \cup \{\ell\})} r^{L \cup \{\ell\}} \quad (46)$$

$$= \sum_{\ell \in \mathbb{L}} r^{(\ell)} \left\langle p^{(\ell)} \ln(K p^{(\ell)}) \right\rangle \sum_{L \subseteq \mathbb{L} \setminus \{\ell\}} \tilde{r}^{(\mathbb{L} \setminus \{\ell\}) \setminus L} r^L \quad (47)$$

$$= \sum_{\ell \in \mathbb{L}} r^{(\ell)} \left\langle p^{(\ell)} \ln(K p^{(\ell)}) \right\rangle. \quad (48)$$

Here, (45) is the result of Lemma 3; (46) is the result of Lemma 1; while (48) is the result of the Binomial Theorem, i.e., $\sum_{L \subseteq \mathbb{L} \setminus \{\ell\}} \tilde{r}^{(\mathbb{L} \setminus \{\ell\}) \setminus L} r^L = (\tilde{r} + r)^{\mathbb{L} \setminus \{\ell\}} = 1$.

Substituting (43) and (48) into (37), we have:

$$h(\mathbf{X}) = - \sum_{\ell \in \mathbb{L}} \left[r^{(\ell)} \ln r^{(\ell)} + \tilde{r}^{(\ell)} \ln \tilde{r}^{(\ell)} + r^{(\ell)} \left\langle p^{(\ell)} \ln(K p^{(\ell)}) \right\rangle \right] \square.$$

Proof of Proposition 2: We want to prove that this mutual information $q_I(\mathbf{A}) \triangleq I(\mathbf{X}; \mathbf{Z}(\mathbf{A}))$ is a monotone submodular set function, that is $\forall \mathbf{A} \subseteq \mathbf{B} \subset \mathbf{A}$ and $\forall \mathbf{a} \in \mathbf{A} \setminus \mathbf{B}$:

$$q(\mathbf{B} \cup \{\mathbf{a}\}) - q(\mathbf{B}) \leq q(\mathbf{A} \cup \{\mathbf{a}\}) - q(\mathbf{A}),$$

$$\Leftrightarrow I(\mathbf{X}; \mathbf{Z}(\mathbf{B} \cup \{\mathbf{a}\})) - I(\mathbf{X}; \mathbf{Z}(\mathbf{B})) \leq I(\mathbf{X}; \mathbf{Z}(\mathbf{A} \cup \{\mathbf{a}\})) - I(\mathbf{X}; \mathbf{Z}(\mathbf{A})).$$

According to (3.53) and (25.36) in [20], we have: $\int \pi_{\mathbf{Z}}(\mathbf{Z}_1 \cup \mathbf{Z}_2) \delta(\mathbf{Z}_1 \cup \mathbf{Z}_2) = \int \pi_{\mathbf{Z}}(\mathbf{Z}_1, \mathbf{Z}_2) \delta \mathbf{Z}_1 \delta \mathbf{Z}_2$. Thus, it is equivalent to

$$I(\mathbf{X}; \mathbf{Z}(\mathbf{B}, \mathbf{Z}(\mathbf{a}))) - I(\mathbf{X}; \mathbf{Z}(\mathbf{B})) \leq I(\mathbf{X}; \mathbf{Z}(\mathbf{A}, \mathbf{Z}(\mathbf{a}))) - I(\mathbf{X}; \mathbf{Z}(\mathbf{A})).$$

Based on the definition i.e., $\mathbf{Z}(\mathbf{A}) = \uplus_{\alpha \in \mathbf{A}} \mathbf{Z}(\alpha)$, and because $\mathbf{A} \subseteq \mathbf{B}$, $\mathbf{a} \in \mathbf{A} \setminus \mathbf{B}$, we have: $\mathbf{Z}(\mathbf{A}) \subseteq \mathbf{Z}(\mathbf{B})$ and $\mathbf{Z}(\mathbf{a}) \in \mathbf{Z} \setminus \mathbf{Z}(\mathbf{B})$. Thus, it is equivalent to proving $\forall \mathbf{R} \subseteq \mathbf{Z} \subseteq \mathbf{Z}$ and $\forall \mathbf{z} \in \mathbf{Z} \setminus \mathbf{Z}$:

$$I(\mathbf{X}; \mathbf{Z}, \mathbf{z}) - I(\mathbf{X}; \mathbf{Z}) \leq I(\mathbf{X}; \mathbf{R}, \mathbf{z}) - I(\mathbf{X}; \mathbf{R}).$$

Since $\mathbf{R} \subseteq \mathbf{Z} \subseteq \mathbf{Z}$, using mutual information inequalities [6, p.50], we have:

$$\begin{aligned} I(\mathbf{Z}; \mathbf{z}) \geq I(\mathbf{R}; \mathbf{z}) &\Leftrightarrow h(\mathbf{z}) - h(\mathbf{z}|\mathbf{Z}) \geq h(\mathbf{z}) - h(\mathbf{z}|\mathbf{R}) \\ &\Leftrightarrow h(\mathbf{z}|\mathbf{R}) \geq h(\mathbf{z}|\mathbf{Z}), \\ &\Leftrightarrow h(\mathbf{R}, \mathbf{z}) - h(\mathbf{R}) \geq h(\mathbf{Z}, \mathbf{z}) - h(\mathbf{Z}). \end{aligned} \quad (49)$$

Further, $I(\mathbf{Z}; \mathbf{z}|\mathbf{X}) = I(\mathbf{R}; \mathbf{z}|\mathbf{X}) = 0$ is due to \mathbf{z} is independent of \mathbf{R} and \mathbf{Z} given \mathbf{X} , we have:

$$\begin{aligned} h(\mathbf{z}|\mathbf{X}) &= h(\mathbf{z}|\mathbf{X}, \mathbf{Z}) + I(\mathbf{Z}; \mathbf{z}|\mathbf{X}) = h(\mathbf{z}|\mathbf{X}, \mathbf{Z}) \\ &= h(\mathbf{X}, \mathbf{Z}, \mathbf{z}) - h(\mathbf{X}, \mathbf{Z}), \\ h(\mathbf{z}|\mathbf{X}) &= h(\mathbf{z}|\mathbf{X}, \mathbf{R}) + I(\mathbf{R}; \mathbf{z}|\mathbf{X}) = h(\mathbf{X}, \mathbf{R}, \mathbf{z}) - h(\mathbf{X}, \mathbf{R}). \end{aligned}$$

Hence

$$h(\mathbf{X}, \mathbf{Z}, \mathbf{z}) - h(\mathbf{X}, \mathbf{Z}) = h(\mathbf{X}, \mathbf{R}, \mathbf{z}) - h(\mathbf{X}, \mathbf{R}). \quad (50)$$

Subtracting (49) from (50), we have:

$$\begin{aligned} [h(\mathbf{X}, \mathbf{Z}, \mathbf{z}) - h(\mathbf{X}, \mathbf{Z})] - [h(\mathbf{Z}, \mathbf{z}) - h(\mathbf{Z})] \\ \geq [h(\mathbf{X}, \mathbf{R}, \mathbf{z}) - h(\mathbf{X}, \mathbf{R})] - [h(\mathbf{R}, \mathbf{z}) - h(\mathbf{R})] \end{aligned}$$

Using differential entropy chain rules [6, p.253], we have that $h(\mathbf{X}|\mathbf{Z}, \mathbf{z}) = h(\mathbf{X}, \mathbf{Z}, \mathbf{z}) - h(\mathbf{Z}, \mathbf{z})$ and $h(\mathbf{X}|\mathbf{Z}) = h(\mathbf{X}, \mathbf{Z}) - h(\mathbf{Z})$, thus the above equation is equivalent to

$$\begin{aligned} h(\mathbf{X}|\mathbf{Z}, \mathbf{z}) - h(\mathbf{X}|\mathbf{Z}) &\geq h(\mathbf{X}|\mathbf{R}, \mathbf{z}) - h(\mathbf{X}|\mathbf{R}) \\ &\Leftrightarrow [h(\mathbf{X}) - h(\mathbf{X}|\mathbf{Z}, \mathbf{z})] - [h(\mathbf{X}) - h(\mathbf{X}|\mathbf{Z})] \\ &\leq [h(\mathbf{X}) - h(\mathbf{X}|\mathbf{R}, \mathbf{z})] - [h(\mathbf{X}) - h(\mathbf{X}|\mathbf{R})], \\ &\Leftrightarrow I(\mathbf{X}; \mathbf{Z}, \mathbf{z}) - I(\mathbf{X}; \mathbf{Z}) \leq I(\mathbf{X}; \mathbf{R}, \mathbf{z}) - I(\mathbf{X}; \mathbf{R}). \end{aligned}$$

Thus, $I(\mathbf{X}; \mathbf{Z}(\mathbf{A}))$ is a *submodular* set function. Further, using the chain rule we have:

$$I(\mathbf{X}; \mathbf{Z}(\mathbf{A}), \mathbf{Z}(\mathbf{a})) - I(\mathbf{X}; \mathbf{Z}(\mathbf{A})) = I(\mathbf{X}; \mathbf{Z}(\mathbf{A})|\mathbf{Z}(\mathbf{a})) \geq 0$$

Hence, $I(\mathbf{X}; \mathbf{Z}(\mathbf{A}))$ is a *monotone submodular* set function of \mathbf{A} \square .